Solutal convection and morphological instability in directional solidification of binary alloys

B. Caroli, C. Caroli, C. Misbah, B. Roulet

J. Physique **46** (1985) 401-413 MARS **1985**, PAGE 401

Classification
Physics Abstracts
47.20 — 64.70D — 61.50C

Solutal convection and morphological instability in directional solidification of binary alloys

B. Caroli (+), C. Caroli, C. Misbah and B. Roulet

Groupe de Physique des Solides de l'Ecole Normale Supérieure (*), Université Paris VII, 2, place Jussieu, 75251 Paris Cedex 05, France

(*Reçu le 24 juillet 1984, accepté le 15 novembre 1984*)

Résumé. — Nous étudions l'effet du couplage entre déformation du front solide-liquide et convection solutale sur la position de la bifurcation à partir de l'état plan quiescent pour un alliage binaire dilué soumis à un processus de solidification directionnelle. Nous développons un traitement de perturbation du couplage entre les bifurcations « nues » — correspondant aux instabilités de Mullins-Sekerka et de convection solutale classiques. Nous montrons que le déplacement de la bifurcation de Mullins-Sekerka est extrêmement faible aux valeurs usuelles du gradient thermique appliqué, et calculable à partir de l'expression de perturbation du 1er ordre. Le déplacement de la bifurcation convective, quoique plus important, peut aussi s'obtenir, dans ce domaine de gradients thermiques, avec une bonne précision, par le calcul au premier ordre. Nous donnons une interprétation qualitative de ces résultats en termes d'un nombre de Rayleigh effectif et de l'écart entre les vecteurs d'onde critiques en l'absence de couplage.

Abstract. — We study the effect of the coupling between front deformation and solutal convection on the position of the bifurcation from the planar quiescent state of a dilute binary alloy submitted to directional solidification. We set up a perturbation treatment of the coupling between the « bare » (Mullins-Sekerka and solutal convective) bifurcations. We show that the shift of the Mullins-Sekerka bifurcation is extremely small at usual values of the applied thermal gradient, and is accurately predicted by the first order perturbation expression. The shift of the convective bifurcation, though much larger, can also be calculated with very good accuracy in the same range of values of the thermal gradient with the help of the first order approximation. We give a qualitative interpretation of these results in terms of an effective Rayleigh number and of the mismatch between the critical wavevectors of the uncoupled system.

1. Introduction.

Binary mixtures submitted to directional solidification (a growth mode in which the solid phase is pulled at an imposed constant velocity V in an external thermal gradient) are well known to exhibit a morphological instability which was first analysed, in the absence of gravity, by Mullins and Sekerka [1] : beyond a threshold velocity, the (previously planar) solid-liquid front develops a periodic « cellular » deformation.

In such a setup, the system is submitted to an external thermal gradient. Moreover, solidification produces, at the interface, an excess (or defect) of solute concentration, the diffusive evacuation of which induces a concentration gradient ahead of the front in the liquid phase. As is well known, in the presence of gravity, each of these gradients induces buoyancy forces which may give rise to a convective instability.

We will only consider the simplest geometry, where the solid is pulled vertically and the melt is not stirred. The three above-mentioned instabilities then give rise to horizontal temperature and concentration gradients which couple the velocity field and the surface deformation. One therefore expects the corresponding bifurcations to feel the influence of this coupling : the Mullins-Sekerka (MS) bifurcation must be shifted by the presence of gravity, while the convective ones must depend on the deformability of the interface.

This question was first raised by Coriell *et al.* [2], then reconsidered by Hurle *et al.* [3] who neglected

(+) Also : Département de Physique, UER de Sciences Exactes et Naturelles, Université de Picardie, 33 rue Saint-Leu, 80000 Amiens.

(*) Associé au CNRS.

thermally-induced convection. This assumption is obviously useful : indeed, the theoretical formulation then becomes much less heavy, which helps to distinguish and analyse the main physical features of the problem. Coriell *et al.* [2] have shown that it is justified, except at very small pulling velocities, if one assumes that the temperature gradient is stabilizing : this means, for most materials — for which $\partial\rho/\partial T < 0$ at the melting temperature — pulling the solid downwards. We will from now on follow Hurle *et al.* [3], and assume that $\partial\rho/\partial T = 0$; i.e., we only consider solutal convective effects, assuming that the solutal-induced buoyancy force is destabilizing.

The complexity of the problem led both Coriell *et al.* [2] and Hurle *et al.* [3] to calculate the position of the coupled bifurcations numerically. It appears that their results exhibit a simple physical feature : they find that the shift of the MS bifurcation due to gravity is very small, except for extremely small values ($< 10^{-2}$ K/cm) of the external temperature gradient.

This naturally leads one to think that the relevant associated physical coupling is weak. Thus, in the present article, we try to develop further the analytic approach to this problem, our aim being to extract the relevant physical parameters in the various regimes, which will enable us to define regions of the parameter space where the effective couplings are small enough for appropriate perturbation expansions to be valid.

In particular, we will prove that, as can be expected, the convective bifurcation is shifted by the coupling — as well as the MS one — contrary to what is implied by the analysis of reference [3].

The physical reason for the weakness of the effective coupling is rather simple. Let us assume that the external thermal gradient is fixed. For mixtures of two given materials, the remaining external parameters are the pulling velocity V and the initial concentration C_∞. One can define, for such systems, two « uncoupled » bifurcations :

(i) the « pure morphological » one, i.e. the MS bifurcation at zero gravity;

(ii) the « pure convective » one, i.e. the convective bifurcation in the liquid phase ahead of a growing solid with a planar non-deformable surface.

These bifurcations correspond, in the (C_∞, V) plane, to two curves (see Fig. 1) which have a single intersection at a « crossing point » $(V_0, C_{\infty,0})$. It is only the regions labelled (1) on figure 1 of these curves which give rise to the curve describing the bifurcation of the real (coupled) system from the planar quiescent state.

At the crossing point, to zeroth order in the coupling, the system has two marginal modes, a convective and a MS one, at wavevectors a_0^* and a_0^{MS} which are *different* (except for one single value of the thermal gradient). At the instability threshold, which is (exactly) obtained from a linear development in the mode

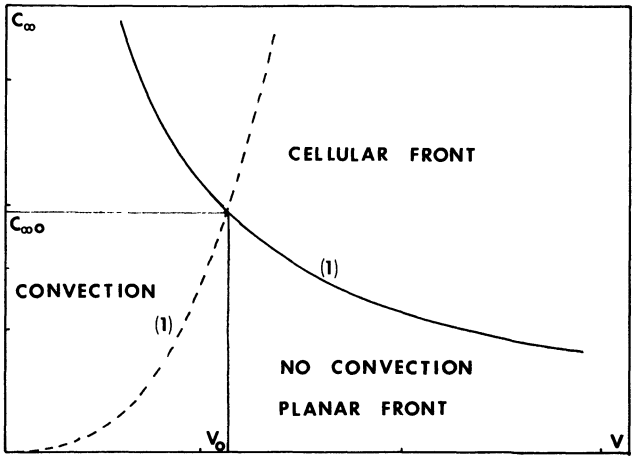

Fig. 1. — Pure Mullins-Sekerka (full line) and pure convective (dashed line) bifurcation curves in the (C_∞, V) plane for a fixed thermal gradient. The regions labelled (1) of these curves (below the crossing point $(C_{\infty 0}, V_0)$) define the zeroth-order approximation of the bifurcation curve of the real system.

amplitudes, only modes with the same wavevector can couple : for example, the zeroth order marginal convective mode only couples with the MS (front deformation) mode of wavevector a_0^*. Since $a_0^* \neq a_0^{MS}$, this MS mode is relaxing, its relaxation rate increasing with the mismatch between a_0^* and a_0^{MS}. That is, the larger this mismatch, the more the MS mode is « slaved » by the convective one, and the smaller the effect of the coupling on the convective mode. We will see that it is only for very small thermal gradients that a_0^* and a_0^{MS} approach each other. For larger, more realistic, thermal gradients, $a_0^{MS}/a_0^* \gg 1$, which reduces the effective coupling.

When V and C_∞ move away from the crossing point along parts (1) of the zeroth-order bifurcation curves, this reduction should become stronger : let us, for example, consider a point on the convective branch. At this point, the zeroth-order system has a single marginal (convective) mode at wavevector a^*. The MS modes are all stable, their relaxation rates must increase, for a given wavevector, with the distance from (V, C_∞) to the crossing point. Therefore, moving away from the crossing point should increase the efficiency of the slaving of the MS mode coupled with the marginal convective one.

In § 2, following reference [3], we rederive the condition of existence of marginal modes in the coupled system. In § 3, the results concerning the uncoupled bifurcations are briefly recalled and analysed. In § 4, we set up the perturbation expansions appropriate to the weak coupling regimes, and calculate explicitly, to first order, the shifts of the bifurcation curves. We show that the first order approximation is justified for not too small thermal gradients. In this regime, which corresponds to commonly realized experimental conditions, it gives

very accurate predictions for the shift values. It is found that the coupling effect is much smaller for the MS than for the convective branch, and that, in this weak coupling regime, the coupling always stabilizes the planar quiescent state. These results are discussed qualitatively in § 4 and 5.

2. The planar quiescent solution and the linearized problem.

We consider the following situation (Fig. 2) : a dilute binary mixture is pulled in the $(-\hat{\mathbf{z}})$ direction at velocity V; the system is quasi-infinite (on the scale of all the wavelengths of interest) in the $(\hat{\mathbf{x}}, \hat{\mathbf{y}})$ horizontal directions.

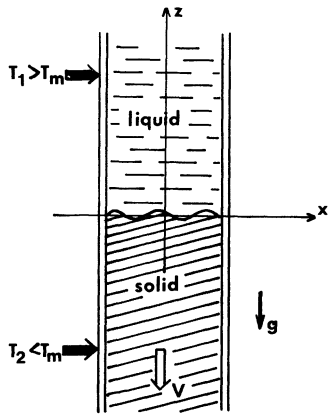

Fig. 2. — Vertical directional solidification setup.

Following references [2, 3], we neglect intrinsic advection, i.e. neglect the difference between the equilibrium densities of the two phases (1).

We use the following dimensionless variables :

$$\begin{aligned} (x, z) &= (\tilde{x}, \tilde{z})/(D/V); \qquad t = \tilde{t}/(D/V^2) \\ (\mathbf{u}, \mathbf{u}_s) &= (\tilde{\mathbf{u}}, \tilde{\mathbf{u}}_s)/V; \qquad T = \tilde{T}/T_M \\ C &= \tilde{C}/(C_\infty/K) \end{aligned} \tag{1}$$

where the tilted variables are the physical ones. $\tilde{T}$, $\tilde{u}$, $\tilde{u}_s$ are respectively the temperature, liquid velocity and front velocity. D is the solute diffusion coefficient in the liquid, T_M the melting temperature of the pure solvent. The solute concentration in the liquid far ahead of the front is assumed to be kept constant. K is the equilibrium solute distribution coefficient ($K = m_L/m_S$, where m_L, m_S are the slopes of the liquidus and solidus curves on the binary phase diagram at $\tilde{T} = T_M$, $\tilde{C} = 0$).

Following the classical analysis of the MS instability [4], since heat diffusion is quasi-instantaneous compared with solute diffusion, we neglect all terms proportional to D/D_{th} (where D_{th} is a heat diffusion coefficient) in the dimensionless equations. Analogously, it must be noticed that kinematic viscosities ν at the melting point are much larger than diffusion coefficients (typically the inverse Schmidt number $Sc^{-1} = D/\nu < 10^{-2}$), i.e. momentum diffusion in the liquid phase is also quasi-instantaneous compared with solute diffusion, and we also neglect terms of order D/ν. Finally, we neglect diffusion in the solid phase, and treat the liquid as incompressible.

The system is then completely described by the following set of equations (equivalent to those of references [2, 3] in the limit $D/D_{th} = D/\nu = 0$).

(i) In the solid phase :

— Heat diffusion :

$$\nabla^2 T_S = 0. \tag{2}$$

(ii) In the liquid phase :

— Heat diffusion :

$$\nabla^2 T_L = 0. \tag{3}$$

— Solute diffusion :

$$\partial C/\partial t = \nabla^2 C + (\hat{\mathbf{z}} - \mathbf{u}).\nabla C \tag{4}$$

where $\hat{\mathbf{z}}$ is the unit vector along Oz.

— Mass conservation :

$$\nabla.u = 0. \tag{5}$$

— Momentum conservation :

$$(\nabla^2)^2 u_z + (gD^2 C_\infty \alpha/\nu V^3 K)(\partial^2/\partial x^2 + \partial^2/\partial y^2).C = 0 \tag{6}$$

where $\alpha = -\rho^{-1} \partial\rho/\partial C$ is the solutal expansion coefficient, and the gravity $g > 0$. Equation (6) is obtained, in the limit $Sc^{-1} = 0$, by twice taking the curl of the Navier-Stokes equation.

(iii) At the interface $(z = z_s(\mathbf{r}, t))$:

— No-slip condition :

$$\mathbf{u} \times \mathbf{n} = 0 \tag{7.a}$$

where $\mathbf{n}$ is the unit vector along the normal to the front pointing into the liquid.

— Mass conservation in the absence of intrinsic advection :

$$\mathbf{u}.\mathbf{n} = 0. \tag{7.b}$$

— Continuity of temperature :

$$T_S = T_L. \tag{8}$$

— Heat balance :

$$n.[\nabla T_L - (k_S/k_L)\nabla T_S] = 0 \tag{9}$$

where $k_{S,L}$ are the thermal conductivities.

— Concentration balance :

$$\nabla C.\mathbf{n} = (K - 1) C\mathbf{u}_s.\mathbf{n}. \tag{10}$$

(1) This effect, which does not introduce any new qualitative feature in the problem, will be studied in a forthcoming article.

— Curvature-induced local interface temperature shift :

$$T_L = 1 + MC - \Gamma\mathcal{K} \quad (11)$$

where $M = m_L C_\infty / KT_M$, $\Gamma = \gamma V/LD$, L being the specific latent heat of fusion and γ the solid-liquid surface tension. $\mathcal{K}$ is the curvature of the front, defined as positive for a convex solid.

As already mentioned, equations (2), (3) neglect the term (D/D_{th}) $(\partial T_{L,S}/\partial t - \partial T_{L,S}/\partial z)$, and equation (9) neglects the latent heat production term (D/D_{th}) $(L/C_p T_M)$ $\mathbf{u}_s \cdot \mathbf{n}$.

This is justified, due to the smallness of D/D_{th}, except if the lengths of interest (here, the wavelength of the front deformation mode D/Va_{MS}, or that of the convective mode D/Va^*) become comparable with the thermal diffusive length D_{th}/V. This can only occur for the MS wavelength, and only at the very large velocities and extremely small thermal gradients corresponding to the immediate vicinity of the upper threshold of the MS bifurcation [4] (typically, V in the m/s range and $G \ll 10^{-2}$ K/cm), a region of parameter space which will not be of interest here.

Finally, equations (10) and (11) assume quasi-instantaneous local thermodynamic equilibrium on the front, which implies that the interface is microscopically rough.

2.1 THE PLANAR QUIESCENT STATIONARY SOLUTION. — Choosing the front position as the origin of the z-coordinate, one easily sees that the above system of equations has a planar quiescent stationary solution :

$$\left.\begin{aligned} C_0(z) &= K + (1 - K)\, e^{-z} \\ T_{L0}(z) &= 1 + M + G_L\, z \quad (z > 0) \\ \mathbf{u}_0 &= 0 \end{aligned}\right\} \quad (12.a), (12.b), (12.c)$$

$$T_{S0}(z) = 1 + M + (G_L/n)\, z \quad (z < 0) \quad (12.d)$$

where $n = k_S/k_L$, and G_L is the (positive) dimensionless temperature gradient in the liquid phase.

2.2 LINEAR STABILITY OF THE PLANAR QUIESCENT STATE. — Let us now assume that the planar front undergoes a small harmonic deformation of wavevector $\mathbf{a}$, the direction of which is chosen to define the x-axis :

$$z_{s1}(x, t) = \zeta \cos(ax)\, e^{\sigma t}. \quad (13)$$

This deformation induces responses $\delta\mathbf{f}(z, x, t)$ (with $\mathbf{f} \equiv (C, T_L, T_S, u_z)$) of the concentration, temperature and velocity fields. Expanding equations (2) to (11) to first order in ζ about the planar quiescent solution, one gets :

$$\delta\mathbf{f}(z, x, t) = \mathbf{f}_1(z) \cos(ax)\, e^{\sigma t}. \quad (14)$$

Equations (2) to (6) then give :

$$\left(\frac{d^2}{dz^2} - a^2\right)^2 u_{1z}(z) - \frac{g\alpha D^2 C_\infty}{\nu K V^3} a^2 C_1(z) = 0 \quad (15.a)$$

$$\left(\frac{d^2}{dz^2} + \frac{d}{dz} - a^2 - \sigma\right) C_1(z) + (1 - K)\, e^{-z} u_{1z}(z) = 0 \quad (15.b)$$

$$\left(\frac{d^2}{dz^2} - a^2\right) T_{L1}(z) = 0 \quad (16.a)$$

$$\left(\frac{d^2}{dz^2} - a^2\right) T_{S1}(z) = 0 \quad (16.b)$$

with [3] :

$$C_1(\infty) = T_{L1}(\infty) = T_{S1}(-\infty) = u_{1z}(\infty) = \left.\frac{du_{1z}}{dz}\right|_{z=\infty} = \left.\frac{d^2u_{1z}}{dz^2}\right|_{z=\infty} = 0. \quad (17)$$

Equations (16.a, b) for the temperature field can be solved trivially, together with the linearized version of interface conditions (8), (9), giving [2, 3] :

$$T_{L1}(z) = \frac{1 - n}{1 + n} G_L\, \zeta\, e^{-az} \quad (18.a)$$

$$T_{S1}(z) = \frac{n - 1}{n(1 + n)} G_L\, \zeta\, e^{+az}. \quad (18.b)$$

Plugging this solution into the linearized interface conditions obtained from equations (7), (10), (11), one gets :

$$u_{1z}(0) = 0 \quad (19.a)$$

$$du_{1z}/dz\,|_{z=0} = 0 \quad (19.b)$$

$$dC_1/dz\,|_{z=0} - (K - 1)\, C_1(0) = (K - 1)(K + \sigma)\,\zeta \quad (19.c)$$

$$MC_1(0) + \left[M(K - 1) - \frac{2 G_L}{1 + n} - \Gamma a^2\right]\zeta = 0. \quad (19.d)$$

Elimination of $C_1(z)$ between equations (15.a) and (15.b) and of ζ between equations (19.c) and (19.d) finally reduces the linear stability problem to solving [3] :

$$\left(\frac{d^2}{dz^2} + \frac{d}{dz} - a^2 - \sigma\right)\left(\frac{d^2}{dz^2} - a^2\right)^2 u_{1z} + R_s a^2 \times e^{-z} u_{1z} = 0 \quad (20)$$

with the boundary conditions :

$$u_{1z}(\infty) = \left.\frac{du_{1z}}{dz}\right|_{z=\infty} = \left.\frac{d^2u_{1z}}{dz^2}\right|_{z=\infty} = 0 \quad (21.a)$$

and :

$$u_{1z}(0) = 0 \quad (21.b)$$

$$du_{1z}/dz\,|_{z=0} = 0 \quad (21.c)$$

$$\left[\frac{d}{dz} - (K - 1) + \frac{K + \sigma}{\mathcal{C} - \beta a^2}\right]\left(\frac{d^2}{dz^2} - a^2\right)^2 u_{1z}\Big|_{z=0} = 0 \quad (21.d)$$

where

$$\mathcal{C} = 1 - \frac{2 G_L}{(1 + n) M(K - 1)}; \quad \beta = \frac{\Gamma}{M(K - 1)}. \quad (22)$$

The Rayleigh number R_s appearing in equation (20) is defined as :

$$R_s = \frac{1 - K}{K} \cdot \frac{g\alpha D^2 C_\infty}{\nu V^3}. \quad (23)$$

We assume it to be positive ($(1 - K)\alpha > 0$), in order to describe a situation which can give rise to a solutal convective instability.

The volume problem is non trivial, due to the presence of the non-constant e^{-z} coefficient. This stems from the exponential shape of the zeroth-order concentration profile, which is characteristic of the diffusion-controlled growth situation. The Rayleigh number defined in equation (23) has the standard form ($R_s \sim g\alpha(\nabla\tilde{C})\, d^4/D\nu$) appropriate to a « Bénard-like convective box » of thickness $d \sim D/V$ with an applied concentration gradient $\nabla\tilde{C} \sim (1 - K) VC_\infty/KD$.

Following Hurle *et al.* [3] ([2]), we express the three independent solutions of equation (20) $U^{(i)}$ ($i = 1, 2, 3$) which satisfy boundary conditions (21.a) in terms of power series of the variable $s = e^{-z}$ (and of Logs). The explicit expressions of the $U^{(i)}$(s) are given in the appendix. The general solution of equation (20) must then satisfy the three interface conditions (21.b, c, d). The resulting compatibility condition provides the dispersion relation for the modes of the linearized system $F(\sigma, a) = 0$.

Since we look for the instability threshold, we are only interested in the condition of existence of neutral modes, defined by Re $\sigma = 0$. We assume at this stage that the principle of exchange of stabilities holds in the system, i.e. that the neutral modes have Im $\sigma = 0$. We will come back in § 5 to the validity of this assumption in the weak coupling limit we are interested in.

The condition of existence of neutral modes can then be written as :

$$B + \left[K - 1 - \frac{K}{\mathcal{C} - \beta a^2}\right] A = 0 \quad (24)$$

with

$$B = \begin{vmatrix} d_{11} & d_{12} & d_{13} \\ d_{21} & d_{22} & d_{23} \\ b_{31} & b_{32} & b_{33} \end{vmatrix} \quad A = \begin{vmatrix} d_{11} & d_{12} & d_{13} \\ d_{21} & d_{22} & d_{23} \\ a_{31} & a_{32} & a_{33} \end{vmatrix} \quad (25)$$

and

$$d_{1i} = U^{(i)}(z = 0, \sigma = 0) \quad (26.a)$$

$$d_{2i} = -\frac{d}{dz} U^{(i)}(z, \sigma = 0)\Big|_{z=0} \quad (26.b)$$

$$b_{3i} = -\frac{d}{dz}\left(\frac{d^2}{dz^2} - a^2\right)^2 U^{(i)}(z, \sigma = 0)\Big|_{z=0} \quad (26.c)$$

$$a_{3i} = \left(\frac{d^2}{dz^2} - a^2\right)^2 U^{(i)}(z, \sigma = 0)\Big|_{z=0}. \quad (26.d)$$

([2]) Note that reference [3] contains various misprints, in particular in its equation (62.b).

The expressions of the d_{ij}, a_{ij}, b_{ij}'s are given in the appendix. It should be noticed that each of them is a power series of the Rayleigh number R_s, the coefficients of which only depend on the (reduced) wavevector **a**.

So, the condition of existence (24) of neutral modes for the system with a deformable front in the presence of gravity appears as a condition linking **a** and the three combinations of the « control parameters » C_∞, $\tilde{G}$, V :

$$R_s = r\frac{C_\infty}{V^3}; \quad \mathcal{C} = 1 - \frac{p\tilde{G}}{VC_\infty}; \quad \beta = \frac{qV}{C_\infty} \quad (27.a)$$

with

$$r = \frac{(1-K)\, g\alpha D^2}{K\nu}; \quad p = \frac{2\, KD}{(1+n)\,(K-1)\, m_L};$$

$$q = \frac{\Gamma K T_M}{(K - 1)\, Dm_L}. \quad (27.b)$$

3. The uncoupled bifurcations.

In order to be able to define weak coupling regimes, we must define uncoupled bifurcations, one of which describes the onset of a purely convective instability, while the other one corresponds to a pure morphological front instability.

3.1 THE PURE MULLINS-SEKERKA BIFURCATION. — Clearly, it can only occur in the absence of gravity. So, the corresponding neutral mode equation is obtained by taking the $R_s = 0$ limit of equation (24). It is found (see appendix) that :

$$B(a; R_s = 0) = m^3; \quad A(a, R_s = 0) = m^2 \quad (28)$$

where :

$$m = \frac{1}{2} + \sqrt{\frac{1}{4} + a^2} \geqslant 1 \quad (29)$$

so that equation (24) reduces to :

$$\mathcal{C} - \beta a^2 - \frac{K}{m + K - 1} = 0 \quad (30)$$

i.e., precisely the MS neutral mode equation [4]. As analysed in detail in reference [4], this equation defines a neutral curve $\mathcal{C} = \mathcal{C}_c(a, \beta)$, and the bifurcation corresponds to the minimum $\mathcal{C}_{MS}$ of $\mathcal{C}_c(a)$, i.e. is determined by the parametric equations (30) and

$$\frac{\partial}{\partial(a^2)} \mathcal{C}_c(a, \beta) \equiv \beta - \frac{K}{(2\, m - 1)\,(m + K - 1)^2} = 0. \quad (31)$$

For fixed $\tilde{G}$ (resp. C_∞) this defines a bifurcation curve in the (C_∞, V) (resp. ($\tilde{G}$, V)) plane. These curves are displayed in figures 1 and 3. Their small-velocity

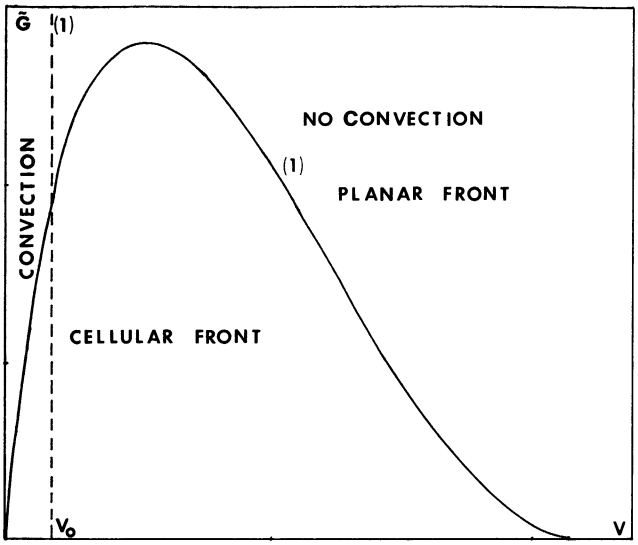

Fig. 3. — Pure Mullins-Sekerka (full line) and pure convective (dashed line) bifurcation curves in the $(\tilde{G}, V)$ plane for a fixed concentration C_∞.

regions are described by the approximate analytic expression :

$$\frac{p\tilde{G}}{VC_\infty} = 1 \tag{32}$$

(up to terms of order $(qV/C_\infty)^{1/3}$). In this region, the critical reduced wavevector (which corresponds to the first neutral mode) is given, to the same order, by :

$$a^{MS} = \left(\frac{KC_\infty}{2qV}\right)^{1/3} \gg 1 . \tag{33}$$

When V increases, the critical wavevector decreases monotonously : at the extremum of the MS bifurcation curve it is, roughly, of order 1, and goes to zero for $V \to C_\infty/qK$.

3.2 THE PURE CONVECTIVE BIFURCATION. — It corresponds to the case of a non-deformable solid-liquid interface, i.e. to the limit of infinite surface tension. So, it is obtained by taking the $\beta \to \infty$ limit of equation (24). The corresponding neutral mode equation reads :

$$B(a, R_s) + (K - 1)\, A(a, R_s) = 0 . \tag{34}$$

For a given material (a given solute distribution coefficient K), equation (34) defines a neutral curve ([3])

$$R_s = R_{sc}(a) \tag{35}$$

([3]) In fact, as usual in convection problems [5], equation (35) only refers to the lowest branch of neutral modes [2] — which describes the convective solution with the smallest number of rolls in the vertical direction.

the minimum of which, (R_s^*, a^*), determines the pure convective bifurcation, thus defined by :

$$R_s \equiv r\frac{C_\infty}{V^3} = R_s^* . \tag{36}$$

Due to the power series form of A and B, equation (34) can only be solved numerically. This has been performed by Hurle, Jakeman and Wheeler [6], for various values of K and of the Schmidt number. We have recalculated $R_s^*(K)$ and $a^*(K)$ for $Sc^{-1} = 0$. Our results are tabulated in table I. They fit closely the values found by Hurle *et al.* [6] for $Sc = 81$. In particular, for the PbSn alloy system, which, following references [2, 3], we will use in the following in all numerical illustrations, $K = 0.3$, and :

$$R_s^* = 10.28 ; \quad a^* = 0.34 . \tag{37}$$

Table I. — *Critical Rayleigh number R_s^* and wavevector a^* for the pure convective bifurcation and coupling coefficient for the convective branch $\xi = (K/R_s^*)\, dR_s^*/dK$ versus distribution coefficient K.*

K	R_s^*	a^*	ξ
0.01	4.47	0.17	0.220
0.02	5.23	0.20	0.230
0.05	6.57	0.25	0.245
0.1	7.88	0.30	0.250
0.2	9.38	0.33	0.249
0.3	10.28	0.34	0.200
0.4	10.87	0.35	0.186
0.6	11.65	0.35	0.154
0.8	12.13	0.35	0.130
1.0	12.46	0.36	0.120
2	13.22	0.36	0.065
3	13.51	0.36	0.049
4	13.66	0.36	0.018

As can be seen in table I and in reference [6], R_s^* increases quite rapidly with K for $K < 0.5$, after which it increases much more slowly. The critical wavevector also increases with K, reaching the quasi-constant value $a = 0.36$ for $K > 0.8$.

The bifurcation is given by equation (36). The bifurcation curves appear as :

— a vertical line in the $(\tilde{G}, V)$ plane, the abscissa of which moves with C_∞ (Fig. 3),

— a cubic curve independent of $\tilde{G}$ in the (C_∞, V) plane (Fig. 1).

Note that the critical wavevector a^* is strictly constant along the pure convective bifurcation curve.

3.3 THE CROSSING POINT OF THE UNCOUPLED BIFURCATION CURVES. — As explained in § 1, it is of interest to determine the crossing point of the two uncoupled

bifurcation curves, and to compare the critical wavevectors a_0^{MS} and a_0^* at this point of parameter space.

Let us assume, to fix ideas, that the thermal gradient $\tilde{G}$ is kept constant, and look for the position $(V_0, C_{\infty 0})$ of the crossing point in the (V, C_∞) plane (Fig. 1). For each value of $\tilde{G}$, there is only one such point.

Let us assume that the value of $\tilde{G}$ is such that $a_0^{MS} \gg 1$. From equation (32), in this regime :

$$C_{\infty 0} \cong \frac{p\tilde{G}}{V_0}. \tag{38}$$

Inserting this expression into equation (36), one gets :

$$V_0 \cong \left(\frac{pr\tilde{G}}{R_s^*}\right)^{1/4} ; \qquad C_{\infty 0} \cong \left(\frac{p^3 R_s^* \tilde{G}^3}{r}\right)^{1/4} \tag{39}$$

and, using equation (33) :

$$a_0^{MS} \cong \left(\frac{K}{2q}\right)^{1/3} \left(\frac{pR_s^* \tilde{G}}{r}\right)^{1/6}. \tag{40}$$

For the PbSn system, for example, using the values of the various parameters given in references [2, 3], this gives (with $\tilde{G}$ in K/cm) :

$$a_0^{MS} \cong \left(\frac{\tilde{G}}{0.02}\right)^{1/6}. \tag{41}$$

The small-velocity approximation (Eqs. (32), (33)) for the MS bifurcation is good for $a \gg 1$. That is, in the PbSn system, for which

$$p = 38.45 \times 10^{-7}\ \text{cm}^2.\text{wt}\,\%/\text{s.K} ;$$
$$q = 61 \times 10^{-3}\ \text{s.wt}\,\%/\text{cm} ;$$
$$r = 4.4 \times 10^{-6}\ \text{cm}^3/\text{s}^3.\text{wt}\,\%,$$

the above expressions (39), (40) for the crossing point parameters and MS-wavevector are valid provided that, in order of magnitude,

$$\tilde{G} \gg 1\ \text{K/cm} \tag{42}$$

and, in this regime :

$$V_0 = 11.36\, \tilde{G}^{1/4}\ (\mu/\text{s}),$$
$$C_{\infty 0} = 3.4 \times 10^{-3}\, \tilde{G}^{3/4}\ (\text{wt}\,\%), \tag{43}$$

(where $\tilde{G}$ is expressed in K/cm).

Note that most experiments are performed in this large gradient regime.

For smaller values of $\tilde{G}$, V_0, $C_{\infty 0}$ and a_0^{MS} must be calculated numerically. They all decrease smoothly with decreasing $\tilde{G}$. In particular, the variation of a_0^{MS} is very slow for small $\tilde{G}$'s. For PbSn, for example, a_0^{MS} only reaches a value close to 1 for $\tilde{G} \simeq 10^{-2}$ K/cm, a quite unrealistically small value in directional growth experiments.

4. The weakly coupled bifurcations.

Equation (24) for the neutral modes of the real system can be exactly rewritten as :

$$\left(\mathcal{C} - \beta a^2 - \frac{K}{m + K - 1}\right)(B + (K - 1)\, A) = \frac{K(mA - B)}{m + K - 1}. \tag{44}$$

In this expression, the r.h.s. term can then be interpreted as a coupling between the pure MS and convective modes defined by equations (30) and (34).

One can now immediately set up a perturbation expansion for the bifurcations of predominantly MS or convective character : one simply has to solve equation (44) formally by successive iterations around each of the uncoupled bifurcations. To first order :

— at the MS-like bifurcation :

$$\delta\mathcal{C} = \left.\frac{K(mA - B)}{(m + K - 1)\,[B + (K - 1)\, A]}\right|_{a = a^{MS}} \tag{45}$$

where

$$\delta\mathcal{C} = \mathcal{C} - \mathcal{C}^{MS} \tag{46.a}$$

$$\mathcal{C}^{MS} = \left[\beta a^2 + \frac{K}{m + K - 1}\right]_{a = a^{MS}} \tag{46.b}$$

— at the convective-like bifurcation :

$$\delta R_s = \frac{KA}{\left[\mathcal{C} - \beta a^2 - \frac{K}{m+K-1}\right]\left[\frac{\partial}{\partial R_s}(B+(K-1)\,A)\right]_{\substack{a=a^* \\ R_s = R_s^*}}} \tag{47}$$

where use has been made of the fact that, for $a = a^*$, $R_s = R_s^*$, equation (34) is satisfied, and

$$\delta R_s = R_s - R_s^*. \tag{48}$$

Note that, to first order, the shift of the critical wavevectors a^{MS}, a^*, does not come into play in expressions (45), (47), due to the fact that they correspond to minima of the zeroth-order $\mathcal{C}_c(a)$ and $R_{sc}(a)$ curves.

Clearly, such first order expansions are valid provided that the relative shifts of the bifurcations are very small, i.e. in the regimes of weak effective couplings.

It can be seen that the effective couplings (which have different values for the two bifurcations) can become small for two different physical reasons :

— the r.h.s. of equation (44) is small, i.e. the « bare » coupling strength is small. As can be seen from equations (28), this is the case, in particular, for small enough R_s,

— one of the two « slaving factors »

$$f_{\text{conv}}(a^{\text{MS}}) = [B + (K - 1)\, A]_{a=a^{\text{MS}}}$$

and

$$f_{\text{MS}}(a^*) = \left[\mathcal{C} - \beta a^2 - \frac{K}{m + K - 1}\right]_{a=a^*}$$

is large. Each of these factors is zero at the corresponding uncoupled bifurcation ($f_{\text{conv}}(a^*) = f_{\text{MS}}(a^{\text{MS}}) = 0$), they increase when the mismatch between a^* and a^{MS} increases. This is related with the corresponding increase in the relaxation rate of the « slaved » mode.

4.1 THE PERTURBED MORPHOLOGICAL BIFURCATION. — Its shift is given, to first order, by equation (45), which must be analysed when the point representing the system moves along that part of the zeroth-order MS bifurcation curve which lies in the (zeroth-order) convection-free region of parameter space. That is, assuming that the thermal gradient $\tilde{G}$ is kept fixed, we are interested in the region $V > V_0$ of the curve. So, one must calculate the values of A and B for the corresponding values $R_s(V)$, $a^{\text{MS}}(V)$ of the Rayleigh number and critical wavevector.

Since the numerical results [2, 3] prove that the r.h.s. of equation (45) is in general small, and since this term vanishes for $R_s = 0$ (Eq. (28)), one may suspect that a small-R_s expansion of A and B will be adequate to calculate the shift of the MS bifurcation.

Consequently, we calculate $A(R_s, a)$ and $B(R_s, a)$ up to terms of first order in R_s. This is done in the appendix. We find that the condition of validity of the small-R_s expansion is different in each of the three regions $a \gg 1$, $a \sim 1$, $a \ll 1$.

— When $a \gg 1$, the expansion parameter is found to be

$$(R_s/a^3)\,(1 + \mathcal{O}(a^{-1}))\,.$$

— For $a \sim 1$, quite obviously, the relevant parameter is R_s itself.

— For $a \ll 1$, the parameter is $R_s\, a^2(1 + \mathcal{O}(a))$.

The first order expansion in each region is satisfactory provided that the corresponding parameter is small.

So, it appears that convective effects are describable in terms of a wavevector-dependent effective Rayleigh number. This is related with the fact that the characteristic length of the convective flow driven by the front deformation is of the order of the wavelength of the deformation, a^{-1}. In particular, in the region $a \gg 1$ [4], where this wavelength is much smaller than the thickness D/V of the diffusion layer, the physically relevant Rayleigh number must be built for a fluid drop of dimension $\sim a^{-1}\, D/V$ (instead of the length D/V used to build R_s) driven by a concentration gradient of order $C_\infty/(a^{-1}\, D/V)$. That is, the effective Rayleigh number is R_s/a^3.

As discussed in § 3.3, for physically reasonable values of $\tilde{G}$, the MS wavevector a_0^{MS} at the crossing point is always > 1. On the other hand, at this point, by definition $R_s = R_s^* \cong 10$. So, clearly, the first order expansion in R_s is valid at the crossing point only if

$$R_s^*/(a_0^{\text{MS}})^3 \ll 1\,. \tag{49}$$

With the help of equation (40), this condition becomes :

$$\frac{2\,q}{K}\left(\frac{rR_s^*}{p\tilde{G}}\right)^{1/2} \ll 1\,. \tag{50}$$

For PbSn, this gives $\tilde{G} \gg 2$ K/cm.

It may be shown, with the help of equations (30), (31) that, when the point representing the system in the (C_∞, V) plane moves away from the crossing point along the MS curve, a^{MS} decreases and

$$R_s = \frac{rq^2}{p\tilde{G}}\,\frac{1 - \mathcal{C}}{\beta^2} \tag{51}$$

decreases monotonously. In the region $a^{\text{MS}} \gg 1$, $R_s \propto V^{-4}$, $a^{\text{MS}} \propto V^{-2/3}$. When $a^{\text{MS}} = 1$, $R_s = rq^2\, \mu/p\tilde{G}$, where μ is a K-dependent number. For PbSn, $R_s(a^{\text{MS}} = 1) = 10^{-1}/\tilde{G}$ (with $\tilde{G}$ in K/cm).

For larger velocities (which are anyhow too large to be easily reached in experiments) $a^{\text{MS}} < 1$, $R_s\, a^2 < R_s(a^{\text{MS}} = 1)$. So, one can conclude that, if the small-R_s expansion is justified at the crossing point (condition (50)), it is valid everywhere along the MS curve, and its accuracy improves with increasing V/V_0. Thus, for not very small temperature gradients, one can safely use the expansion of A and B to first order in R_s (see appendix). From this and equation (45), one gets :

$$\delta\mathcal{C} = \left.\frac{KR_s(m - 1)}{2\,m^2(m+K-1)^2\,(2\,m+2\,a-1)^2}\right|_{a=a^{\text{MS}}} \tag{52}$$

where m is defined by equation (29).

From equation (52), the equation of the shifted bifurcation can be written as :

$$\mathcal{C} \equiv 1 - \frac{p\tilde{G}}{VC_\infty} = \mathcal{C}_c(\beta, a^{\text{MS}}(\beta)) + \delta\mathcal{C} \tag{53}$$

from which one gets, using equation (27.a) for β, at fixed $\tilde{G}$, V (i.e. in the representation of Fig. 1)

$$\left.\frac{\delta C_\infty^{\text{MS}}}{C_\infty}\right|_{V,\tilde{G}} = \frac{\delta\mathcal{C}}{1 - \mathcal{C}_c + \beta(a^{\text{MS}})^2} = \frac{rq^2}{2\,Kp\tilde{G}} \times$$

$$\times \left.\frac{(m-1)^2\,(2\,m-1)\,(m+K-1)\,(2\,m+K-1)}{m^2(2\,m+2\,a-1)^2}\right|_{a=a^{\text{MS}}}. \tag{54}$$

(4) For $a \ll 1$, the physical interpretation of the parameter $R_s\, a^2$ is less clear : it results from a more subtle interplay between the scale $a^{-1}\, D/V$ of the flow and the diffusion length D/V over which the liquid is driven by the buoyancy force.

It is seen from equation (54) that the C_∞-shift is always positive. That is, the coupling to convection stabilizes the planar front. This was to be expected on the basis of the interpretation proposed in § 1. Indeed, the weakly coupled convective mode must be dragged by the MS mode, which is thereby slowed down.

Since we consider $\tilde{G}$'s such that $a_0^{MS} \gg 1$, expression (54) can be expanded in powers of a^{-1}, yielding :

$$\left.\frac{\delta C_\infty^{MS}}{C_\infty}\right|_{V_0,\tilde{G}} \cong \frac{K R_s^*}{32 (a_0^{MS})^5} = \frac{(R_s^*)^{1/6}}{16} \left(\frac{rq^2}{p\tilde{G}}\right)^{5/6} \left(\frac{2}{K}\right)^{2/3} \tag{55}$$

which gives, for PbSn :

$$\left.\frac{\delta C_\infty^{MS}}{C_\infty}\right|_{V_0,\tilde{G}} \cong \left(\frac{12 \times 10^{-4}}{\tilde{G}}\right)^{5/6}. \tag{56}$$

In the vicinity of the crossing point, as long as $a^{MS} \gg 1$,

$$\left.\frac{\delta C_\infty^{MS}}{C_\infty}\right|_{V,\tilde{G}} \cong \left.\frac{\delta C_\infty^{MS}}{C_\infty}\right|_{V_0,\tilde{G}} \left(\frac{V_0}{V}\right)^{2/3}. \tag{57}$$

So, in this weak coupling regime, the relative shift decreases when the representative point of the system moves away from the crossing point along the MS curve. For a given $\tilde{G}$, it is maximum at this point. It is seen from equation (56) that, as soon as $\tilde{G} > 1$ K/cm, $\delta C_\infty^{MS}/C_\infty < 4 \times 10^{-3}$. This perturbation result, which is consistent with the numerical results of references [2, 3], shows that, in practice, the convection-induced shift of the MS bifurcation is negligibly small. It is only at very small thermal gradients (typically $\tilde{G} < 1$ K/cm) that this result would cease to be valid, and that the shift should be calculated numerically [3].

4.2 THE PERTURBED CONVECTIVE BIFURCATION. — To first order in the coupling to front deformation, its shift is given by equation (47). In order to calculate this shift explicitly, we need to know the quantities $A^* = A(R_s^*, a^*)$, $(\partial A/\partial R_s)^*$, $(\partial B/\partial R_s)^*$; a^* and R_s^* are constant along the zeroth-order convective bifurcation curve, and only depend on the distribution coefficient K.

Note that these quantities cannot be computed from a small-R_s expansion : indeed, $R_s^* \simeq 10$, while $a^* \simeq 0.35$ (see § 3.2). So, the relevant parameter in the R_s-expansion of A, B is of order $R_s^* a^{*2} \sim 1$, and these numbers must be calculated numerically.

Expression (47) may be simplified further : $a^*(K)$ and $R_s^*(K)$ are defined by (see § 3.2) :

$$[B + (K - 1) A]_{R_s^*, a^*} = 0, \tag{58.a}$$

$$\frac{\partial}{\partial a}[B + (K - 1) A]_{R_s^*, a^*} = 0. \tag{58.b}$$

Differentiating equation (58.a) with respect to K, and using equation (58.b), one gets :

$$\left.\frac{A}{\frac{\partial}{\partial R_s}[B + (K - 1) A]}\right|_{R_s^*, a^*} = -\frac{dR_s^*}{dK} \tag{59}$$

and equation (47) becomes :

$$\frac{\delta R_s}{R_s^*} = \xi \left[\beta a^{*2} + \frac{K}{m^* + K - 1} - \mathcal{C}\right]^{-1} \tag{60.a}$$

with

$$\xi = \frac{K}{R_s^*} \frac{dR_s^*}{dK}. \tag{60.b}$$

The variation of the coefficient ξ with K is tabulated in table I and plotted on figure 4. For $K = 0.3$ (the value appropriate to the PbSn system), $\xi = 0.20$. It is seen that ξ is always positive and smaller than 0.3, and decreases at large K (this is to be related with the corresponding shrinking of the bare MS bifurcation curve).

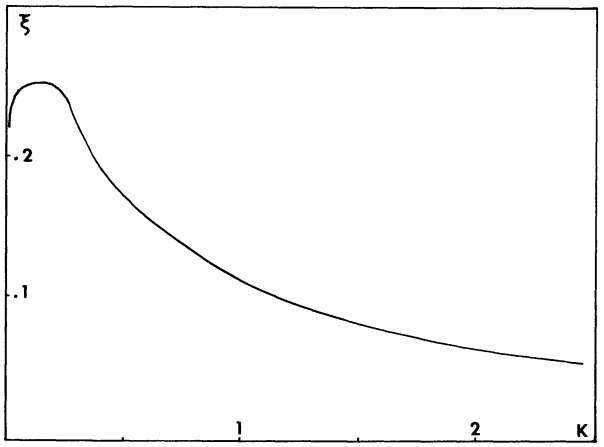

Fig. 4. — The coupling coefficient for the convective branch $\xi = (K/R_s^*)\, dR_s^*/dK$ *versus* distribution coefficient K.

The shift of the zeroth-order convective curve is thus given, with the help of equation (27), by ([5]) :

$$\left.\frac{\delta V(c)}{V}\right|_{C_\infty,\tilde{G}} = -\frac{\xi}{3}\left[\frac{pr\tilde{G}}{R_s^* V^4} + \frac{qra^{*2}}{R_s^* V^2} - \frac{m^* - 1}{m^* + K - 1}\right]^{-1}. \tag{61}$$

([5]) Due to the cubic shape of the zeroth order curve, the approximate value of the V-shift must be more accurate than that of the C_∞-shift.

One can easily show [7], with the help of equations (60), (30), (31), that, at the crossing point :

$$\left[\frac{\delta V^{(c)}}{V}\bigg|_{C_{\infty 0},\tilde{G}}\right]^{-1} = = -\frac{3K}{\xi}\frac{(m_0^{MS}-m^*)^2(2m_0^{MS}+m^*+K-2)}{(m^*+K-1)(2m_0^{MS}-1)(m_0^{MS}+K-1)^2} \quad (62)$$

i.e., at this point, the shift is negative. It is thus clear from equation (61) that $(\delta V^{(c)}/V)_{C_\infty,\tilde{G}}$ retains the same sign for all $V < V_0$.

Moreover, it can easily be checked that the r.h.s. of equation (62) is minimum (and vanishes) for $a_0^{MS} = a^*$ (i.e. $m_0^{MS} = m^*$). That is, as predicted in § 1, the perturbation expansion cannot be valid at the crossing point if the wavevectors of the two marginal modes are not well spaced. In the physical region, where $\tilde{G}$ is not extremely small, $a_0^{MS} > a^*$, and, at large $\tilde{G}$'s ($a_0^{MS} \gg 1$)

$$\frac{\delta V^{(c)}}{V}\bigg|_{C_{\infty 0},\tilde{G}} \cong -\frac{\xi(m^*+K-1)}{3K}. \quad (63)$$

So, the magnitude of the shift at the crossing point is always larger than $\xi/3$. For PbSn ($K = 0.3$), equation (63) gives a value of the order of 9 %.

It is clear from equation (61) that the shift decreases rather rapidly when V decreases, i.e. when the representative point of the system moves away from the crossing point along the convective curve. For example, for PbSn at $\tilde{G} = 200$ K/cm, when $V = 30$ μ/s ($V/V_0 \sim 0.7$), the relative shift predicted by equation (61) is of order 1.8 %.

Therefore, one can conclude that the accuracy of the perturbative expression (61) should be quite good except possibly in the vicinity of the crossing point. In order to check its validity in more detail, we have calculated $(\delta V^{(c)}/V)$ numerically for PbSn from the exact equation (44), following a procedure similar to that of reference [2]. The perturbative and numerical results are plotted on figure 5, in the (C_∞, V) representation for $\tilde{G} = 200$ K/cm and, in the $(\tilde{G}, V)$ representation, for $C_\infty = 0.2$ wt %. The agreement between the perturbative and computed results is very good : we find that the difference, for given C_∞, $\tilde{G}$, between the two values of the velocity never exceeds $\simeq 0.2$ μ/s, while the numerical error may be evaluated to be of the order of 0.1 μ/s. Of course, the quality of this fit may be to a certain extent accidental : one cannot exclude that second order corrections are non negligible, especially in the vicinity of the crossing point, where the shift is largest. However, these results indicate that, although the convective shift is larger than the MS one, the first order perturbation approximation is quite satisfactory for both branches.

One must notice, at this stage, that our results for the shift of the convective bifurcation, while agreeing with the calculations of Coriell *et al.* [2], contradict the analysis of reference [3], which implies that $\delta V^{(c)}$

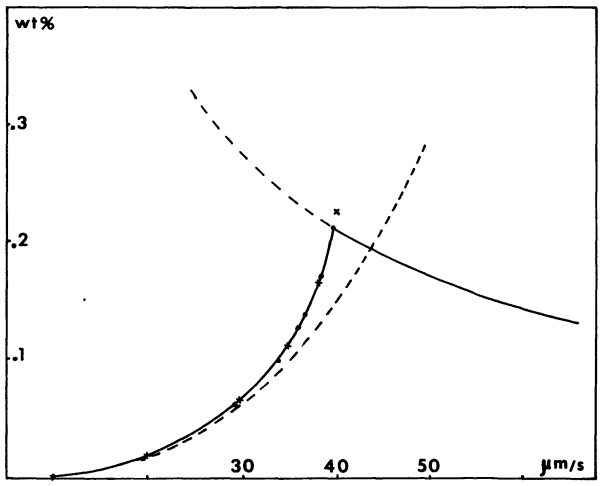

a)

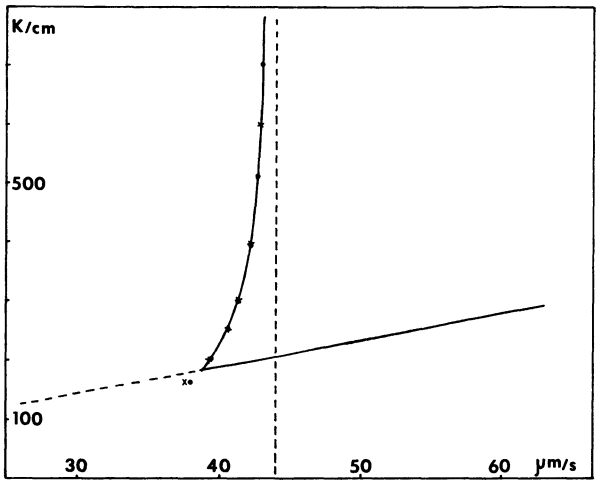

b)

Fig. 5. — Bifurcation curve for the PbSn system. Dashed line : bare bifurcation as in figure 1. Full line : bifurcation of the coupled system. The dots correspond to the perturbative result, the crosses to numerically computed values. *a)* In the (C_∞, V) plane, for a fixed thermal gradient $\tilde{G} = 200$ K/cm. *b)* The vicinity of the crossing point in the $(\tilde{G}, V)$ plane for a fixed concentration $C_\infty = 0.2$ wt %. Note that the shift of the MS curve ($\simeq 10^{-5}$ wt % at the crossing point) is too small to be discernible on the scale of the drawing.

should be strictly zero. We believe that this discrepancy results from the following error in Hurle *et al.*'s work : while their representation of the neutral curve of the coupled system agrees with that of reference [2] and with our calculations, it can be proved that their stability prescription in the region $R_s > R_{sc}(a)$ (see our Eq. (35); this region is the upper part of the band between the dashed lines on Fig. 4 of Ref. [3]) should be inverted. Indeed, large $\tilde{G}$'s, as can be seen from equation (14), are formally equivalent to large β's, i.e., in this limit, MS effects are negligible, and the linear stability of the system is that of the pure convective

one. Since $R_s > R_{sc}(a)$, it is therefore an unstable region, and the minimum of the $G_L(a)$ curve (Fig. 4 of Ref. [3]) does describe the shifted convective bifurcation in the $(\tilde{G}, V)$ representation.

5. Conclusion.

The above perturbative analysis thus appears both qualitatively enlightening and quantitatively accurate at not too small thermal gradients.

On the one hand, it permits one to identify the physical parameters relevant to the problem. On the other hand, it provides a method for calculating analytically the bifurcation shifts due to the coupling between convection and front deformation.

The most striking feature of the results is probably the difference between the orders of magnitude of the shifts of the two bifurcations. The shift of the convective bifurcation is much larger than that of the MS one, and is relatively large in the vicinity of the crossing point.

This difference, as already pointed out, may be traced back to two different sources :

(i) The respective values of the « bare coupling » of equation (44). For the MS case, it is proportional to the *effective* Rayleigh number defined in § 4.1, which decreases as $(R_s/(a_0^{MS})^3)$ for large enough $\tilde{G}$. In the convective case, it is a constant, ξ, which only depends on the distribution coefficient K of the mixture. In practice, it is < 0.3 and decreases with increasing K.

(ii) The « slaving » factors which describe how fast the slaved mode adapts to the marginal one. In the MS case, this factor decreases when a_0^{MS} increases, as can be naively expected, and tends to zero for $a_0^{MS} \gg 1$. In the convective case, it does decrease when the mismatch $(a_0^{MS} - a^*)$ increases, but tends to a finite value of order 1 when $a_0^{MS} \to \infty$. This is due to the fact that the relaxation rate of the pure MS mode, at the bifurcation, is given (6), for $a \cong a_0^{MS}$, by :

$$\sigma^{MS}(a) \cong - \frac{3K}{2(a_0^{MS})^2}(a - a_0^{MS})^2 . \qquad (64)$$

That is, the larger a_0^{MS}, the flatter the $\sigma^{MS}(a)$ curve, and, for $a \cong a^* \ll a_0^{MS}$, $\sigma^{MS}(a^*) \simeq - 3K/2$. The decrease in the curvature of $\sigma^{MS}(a)$ thus roughly compensates for the increase in the mismatch, which limits the slaving effect.

So, at the crossing point, for large $\tilde{G}$'s ($\gg 1$ K/cm), which are commonly used in the experiments, both effects cooperate to give a negligibly small shift of the MS bifurcation, while that of the convective one, of order ξ, is in general not very small. The shifts decrease rapidly when the system moves away from the crossing point along both branches. Their magnitudes increase when the thermal gradient decreases. However, it would take very small $\tilde{G}$'s (typically $\ll 1$ K/cm [3]) for the MS shift to become noticeable, even close to the crossing point. Such small homogeneous thermal gradients seem hardly realizable in practice. Moreover, the corresponding concentrations would be very small (typically, for $\tilde{G} \lesssim 10^{-2}$ K/cm, $C_\infty \lesssim 10^{-4}$ %).

Finally, it is found that, in the perturbative regimes, the coupling is always stabilizing, which expresses the fact that the mode driven by the marginal one is, in the weak coupling limit, always rapidly relaxing.

These results rely on the assumption that the nature of the bifurcations is not affected by the coupling; the uncoupled bifurcations satisfy the principle of exchange of stabilities [4, 6], that is, at the bifurcation, Im $\sigma = 0$ (σ being the relaxation rate). We have assumed, in equation (24), that this remains true for the weakly coupled system, i.e. that the bifurcations do not become of the Hopf type. We have no analytical proof that the principle of exchange of stabilities always holds in the coupled system, but its validity in the weak coupling regime can be inferred from two arguments :

— Coriell *et al.* [2, 8] and Hurle *et al.* [3] have investigated numerically the possibility of the appearance of a Hopf bifurcation for $\tilde{G} = 200$ K/cm in PbSn. They find that, at all V's, Im $\sigma = 0$ at the bifurcation.

— As long as the first order perturbation expansions are valid, an analogous first order calculation can be used to show that there exists a vicinity of the bifurcations in which σ remains real. Let us insist, however, that this is only a weak coupling argument. Indeed, in the vicinity of the point where the uncoupled dispersion curves $\sigma^{MS}(a)$, $\sigma^{(c)}(a)$ cross, a gap in general opens in the dispersion curve of the coupled system, which may correspond to the appearance of a domain of a with no mode with real σ, i.e. to the appearance of two modes with Im $\sigma \neq 0$. This is reflected in the existence of oscillating neutral modes found in references [2, 3] above the bifurcation. When the coupling is weak, this only affects a small region in the (σ, a) space far from the marginal points, where Im σ remains zero. When the coupling strength increases, i.e. at smaller values of $\tilde{G}$ and in the vicinity of the crossing point $(V_0, C_{\infty 0})$, this strong coupling effect might induce the appearance of a Hopf bifurcation. Since the effective coupling is much stronger on the convective branch, it should be the convective bifurcation which will change character first. More numerical calculations at small thermal gradients are needed to check whether this may effectively occur.

We have also neglected thermally-induced convective effects. As shown by Coriell *et al.* [9], when the

(6) Equation (64) can be obtained by expanding the MS dispersion relation [4] :

$$\mathcal{C} - \beta a^2 = \frac{K + \sigma}{K - \frac{1}{2} + \sqrt{\frac{1}{4} + a^2 + \sigma}}$$

at the bifurcation, in powers of σ and $(a - a^{MS})$.

thermal gradient is stabilizing, the effect of thermal expansion on the shift of the solutal convective bifurcation is non negligible only at small velocities (Fig. 2 of Ref. [9]), which can be understood when one notices that the relevant solutal and thermal Rayleigh numbers are such that $R_s \propto V^{-3}$, and $R_{th} \propto V^{-4}$.

Finally, it should be mentioned that the system we have studied — a growing solid with a deformable front in the presence of destabilizing solutal convection — opens a possibility of experimental access to a bifurcation of codimension 2 — a situation in which two different modes become simultaneously unstable. Such a situation is met, for a given value of the thermal gradient, at the crossing point $(V_0, C_{\infty 0})$ of the convective and MS branches. As has been established by bifurcation theory [10], beyond such a bifurcation, a variety of dynamical behaviours can be met, depending on the respective amplitudes of the different nonlinear terms. The present system should be a good candidate to explore such effects, since the ratio between the marginal wavevectors a_0^{MS}, a_0 can be varied in a rather wide range by changing one of the three external parameters, for example the applied thermal gradient.

Appendix

In order to solve equations (15), we apply the operator $\left(\frac{d^2}{dz^2} + \frac{d}{dz} - a^2 - \sigma\right)$ to equation (15.a), and get :

$$\left(\frac{d^2}{dz^2} + \frac{d}{dz} - a^2 - \sigma\right)\left(\frac{d^2}{dz^2} - a^2\right)^2 u_{1z}(z) + R_s a^2 e^{-z} u_{1z}(z) = 0. \quad (A.1)$$

We set $s = e^{-z}$. The three independent solutions $U^{(i)}(s)$ $(i = 1, 2, 3)$ of equation (A.1) which satisfy the boundary conditions (17) at $s = 0$ $(z \to \infty)$ can be calculated with the help of standard power series expansion techniques [11]. One finds :

$$U^{(1)}(s) = s^a + \sum_{n=1}^{\infty} s^{n+a}(- R_s a^2)^n C_n \quad (A.2)$$

$$U^{(2)}(s) = s^a \operatorname{Log} s + \sum_{n=1}^{\infty} s^{a+n}(- R_s a^2)^n C_n[\operatorname{Log} s - W_n] \quad (A.3)$$

$$U^{(3)}(s) = s^\mu + \sum_{n=1}^{\infty} s^{\mu+n}(- R_s a^2)^n B_n \quad (A.4)$$

where

$$\mu = \frac{1}{2} + \sqrt{\frac{1}{4} + a^2 + \sigma} \quad (A.5)$$

and

$$C_n = \left[\prod_{j=1}^{n} j^2(j+2a)^2 (j+a-\mu)(j+a+\mu-1)\right]^{-1} \quad (A.6)$$

$$W_n = \sum_{j=1}^{n}\left[\frac{2}{j} + \frac{2}{j+2a} + \frac{1}{j+a-\mu} + \frac{1}{j+a+\mu-1}\right] \quad (A.7)$$

$$B_n = \left[\prod_{j=1}^{n} j(j+\mu-a)^2 (j+\mu+a)^2 (j+2\mu-1)\right]^{-1}. \quad (A.8)$$

Note that the presence of the Log (s) terms in expression (A.3) for $U^{(2)}(s)$ follows from our approximation $Sc^{-1} = 0$, which results in the degeneracy of two roots of the indicial equation associated with equation (A.1).

From the expressions of the $U^{(i)}$'s (Eqs. (A.2-4)) one immediately obtains the elements of the determinants A, B, defined in equations (25), (26), as :

$$d_{11} = 1 + \sum_{n=1}^{\infty} (- R_s a^2)^n C_n \quad (A.9)$$

$$d_{21} = a + \sum_{n=1}^{\infty} (- R_s a^2)^n (a + n) C_n \quad (A.10)$$

$$b_{31} = \sum_{n=1}^{\infty} (- R_s a^2)^n n^2(n + 2a)^2 (a + n) C_n \quad (A.11)$$

$$a_{31} = \sum_{n=1}^{\infty} (- R_s a^2)^n n^2(n + 2a)^2 C_n \quad (A.12)$$

$$d_{12} = - \sum_{n=1}^{\infty} (- R_s a^2)^n C_n W_n \quad (A.13)$$

$$d_{22} = 1 + \sum_{n=1}^{\infty} (- R_s a^2)^n C_n[1 - (n + a) W_n] \quad (A.14)$$

$$b_{32} = \sum_{n=1}^{\infty} (- R_s a^2)^n C_n n(n + 2a) \times \{ n(n+2a)[1-(n+a) W_n] + 4(n+a)^2 \} \quad (A.15)$$

$$a_{32} = \sum_{n=1}^{\infty} (- R_s a^2)^n C_n n(n + 2a) \times [4(n + a) - n(n + 2a) W_n] \quad (A.16)$$

$$d_{13} = 1 + \sum_{n=1}^{\infty} (- R_s a^2)^n B_n \quad (A.17)$$

$$d_{23} = m + \sum_{n=1}^{\infty} (- R_s a^2)^n B_n(n + m) \quad (A.18)$$

$$b_{33} = m^3 + \sum_{n=1}^{\infty} (- R_s a^2)^n B_n(n + m) \times [n(n + 2m) + m]^2 \quad (A.19)$$

$$a_{33} = m^2 + \sum_{n=1}^{\infty} (- R_s a^2)^n B_n[n(n + 2m) + m]^2 \quad (A.20)$$

where

$$m \equiv \mu(\sigma = 0) = \frac{1}{2} + \sqrt{\frac{1}{4} + a^2} \qquad (A.21)$$

and B_n, C_n, W_n must be calculated at $\sigma = 0$ (i.e. with $\mu \to m$).

Developing A and B (Eq. (25)) up to first order in R_s with the help of equations (A. 9-20), one finds :

$$A = m^2 - R_s a^2\left[\frac{1}{2m} - \frac{m^2(1 + 6a + 4a^2)}{a^2(1 + 2a)^3} - \frac{1}{a} + \frac{(m - a)(1 + 2a)}{a^2}\right] + \mathcal{O}(R_s^2) \qquad (A.22)$$

$$B = m^3 - R_s a^2\left[\frac{m + 1}{2m} - \frac{m + 1}{a} + \frac{(m - a)(a + 1)(2a + 1)}{a^2} - \frac{m^3(1 + 6a + 4a^2)}{a^2(1 + 2a)^3}\right] + \mathcal{O}(R_s^2). \qquad (A.23)$$

In the region $a \gg 1$, equations (A.22), (A.23) may be developed in powers of a^{-1}, which gives :

$$A = a^2\left\{[1 + \mathcal{O}(a^{-2})] - \frac{3R_s}{16a^3}[1 + \mathcal{O}(a^{-1})]\right\} + \mathcal{O}(R_s^2) \qquad (A.24)$$

$$B = a^3\left\{[1 + \mathcal{O}(a^{-2})] - \frac{3R_s}{16a^3}[1 + \mathcal{O}(a^{-1})]\right\} + \mathcal{O}(R_s^2). \qquad (A.25)$$

For $a \ll 1$:

$$A = [1 + \mathcal{O}(a^2)] - \frac{11R_s a^2}{2}(1 + \mathcal{O}(a)) + \mathcal{O}(R_s^2) \qquad (A.26)$$

$$B = [1 + \mathcal{O}(a^2)] - 6R_s a^2(1 + \mathcal{O}(a)) + \mathcal{O}(R_s^2). \qquad (A.27)$$

In order to calculate the shift of the MS bifurcation, as given by equation (45), we need to calculate $mA - B$ in the region $a \gg 1$. It is seen that, to the order in a^{-1} used in equations (A.24), (A.25), mA and B compensate exactly. One must therefore expand the term of order R_s one step further in a^{-1}. This is most easily performed by first calculating $mA - B$ from equations (A.22), (A.23). Using repeatedly the relation $m^2 - m - a^2 = 0$, one gets :

$$mA - B = R_s\frac{(m - 1)}{2(2m + 2a - 1)^2} + \mathcal{O}(R_s^2) \qquad (A.28)$$

from which equation (52) results immediately, and, for $a \gg 1$,

$$mA - B \cong \frac{R_s}{32a}. \qquad (A.29)$$

In order to check that, for $a \gg 1$, the relevant expansion parameter for $mA - B$ is indeed (R_s/a^3) (inspite of the above-mentioned cancellation of lowest order terms), we have calculated the term of order R_s^2 in $mA - B$ of lowest order in a^{-1}. We find that it is effectively of order R_s^2/a^4.

References

[1] MULLINS, W. W. and SEKERKA, R. F., *J. Appl. Phys.* **35** (1964) 444.

[2] CORIELL, S. R., CORDES, M. R., BOETTINGER, W. J. and SEKERKA, R. F., *J. Cryst. Growth* **49** (1980) 13.

[3] HURLE, D. T. J., JAKEMAN, E. and WHEELER, A. A., *J. Cryst. Growth* **58** (1982) 163.

[4] WOLLKIND, D. J. and SEGEL, L. A., *Philos. Trans. R. Soc.* **268** (1970) 351.

[5] CHANDRASEKHAR, S., *Hydrodynamic and Hydromagnetic Stability*, Chap. 2 (Dover New York) 1981.

[6] HURLE, D. T. J., JAKEMAN, E. and WHEELER, A. A., *Phys. Fluids* **26** (1983) 624.

[7] GRAHAM, C. D., *Metal Progr.* **71** (1957) 75.

[8] CORIELL, S. R. and SEKERKA, R. F., *Physicochem. Hydrodynamics* **2** (1981) 281.

[9] MCFADDEN, G. B., REHM, R. G., CORIELL, S. R., CHUCK, W. and MONISH, K. A. (preprint).

[10] GUCKENHEIMER, J. and HOLMES, P. J., *Non Linear Oscillations, Dynamical Systems and Bifurcations of Vector Fields*, Appl. Math. Sciences Series (Springer Berlin) 1983.

[11] WHITTAKER, E. T. and WATSON, G. N., *A Course of Modern Analysis*, Chap. 10 (Cambridge Univ. Press) 4th edition, 1952.